PLANT SCIENCE

Distinct phases of Polycomb silencing to hold epigenetic memory of cold in *Arabidopsis*

Hongchun Yang,[1]* Scott Berry,[1,2]* Tjelvar S. G. Olsson,[2] Matthew Hartley,[2] Martin Howard,[2]† Caroline Dean[1]†

Gene silencing by Polycomb complexes is central to eukaryotic development. Cold-induced epigenetic repression of *FLOWERING LOCUS C* (*FLC*) in the plant *Arabidopsis* provides an opportunity to study initiation and maintenance of Polycomb silencing. Here, we show that a subset of Polycomb repressive complex 2 factors nucleate silencing in a small region within *FLC*, locally increasing H3K27me3 levels. This nucleation confers a silenced state that is metastably inherited, with memory held in the local chromatin. Metastable memory is then converted to stable epigenetic silencing through separate Polycomb factors, which spread across the locus after cold to enlarge the domain that contains H3K27me3. Polycomb silencing at *FLC* thus has mechanistically distinct phases, which involve specialization of distinct Polycomb components to deliver first metastable then long-term epigenetic silencing.

Chromatin-based epigenetic memory is all or nothing, with chromatin modifications propagating bistable states of gene expression (*1*–*4*). One example is silencing of the floral repressor gene *FLOWERING LOCUS C* (*FLC*) in response to prolonged cold (*5*), a process known as vernalization. This involves individual *FLC* loci switching from an active to a stably repressed state in response to cold. This switching requires the conserved Polycomb repressive complex 2 (PRC2) and occurs in two steps: first, nucleation of H3K27me3 in a Polycomb response element (PRE)–like region of two or three nucleosomes close to the *FLC* transcription start site during cold exposure; and second, spreading of H3K27me3 over the entire 7-kb *FLC* locus when plants are returned to the warm. Full coverage with H3K27me3 is associated with long-term epigenetic silencing, and DNA methylation is not involved (*6*). Molecular and genetic studies have identified much of the machinery required for *FLC* epigenetic silencing, but how different factors interact dynamically in relation to the key events of nucleation and spreading has yet to be determined.

The key molecular players involved in *FLC* epigenetic silencing are the PRC2 subunit VERNALIZATION 2 [VRN2, a SU(Z)12 homolog], the plant-homeodomain proteins VERNALIZATION INSENSITIVE 3 (VIN3) and VERNALIZATION 5 (VRN5), the H3K27me3 methyltransferases CURLY LEAF (CLF) and SWINGER (SWN), and the H3K27me3-binding protein LIKE HETEROCHROMATIN PROTEIN 1 (LHP1) (*7*–*12*). To dissect the requirement for these proteins during various stages of *FLC* silencing, we measured *FLC* expression in wild-type (Col-*FRI*) and *vin3*, *vrn2*, *vrn5*, *lhp1*, and *clf* mutants (in a *FRI* background). *vin3*, *vrn2*, and *vrn5* mutants all showed impaired *FLC* shutdown during cold exposure and reactivation after cold (Fig. 1A and fig. S1) (*8*–*10*). By contrast, *FLC* repression in *lhp1* and *clf* mutants was unaffected at the end of cold exposure but was unstable; repression was lost over 20 days after transfer to warm conditions (Fig. 1A and fig. S1). *VIN3* is up-regulated during cold exposure (*9*); however, its expression profile was unchanged from wild-type in the other mutant backgrounds (fig. S2A), indicating that altered *VIN3* expression does not underlie the failure to stably silence *FLC*. The remaining factors *VRN2*, *VRN5*, *SWN*, *CLF*, and *LHP1* are not dynamically regulated during vernalization (fig. S2, B to D) (*10*).

Next, we measured with chromatin immunoprecipitation (ChIP) H3K27me3 and H3K36me3 levels across the *FLC* locus in *vin3*, *vrn2*, *lhp1*, and *clf* mutants. Wild-type plants show accumulation of H3K27me3 and loss of H3K36me3 at the nucleation region during the cold (Fig. 1, B and C, and fig. S3) (*13*, *14*). H3K27me3 nucleation was disrupted in *vin3* and *vrn2* mutants. *lhp1* and *clf* mutants, on the other hand, showed efficient nucleation—disagreeing with a reported role for LHP1 in nucleation (*15*). *lhp1* and *clf* mutants failed to spread H3K27me3 at high levels across the *FLC* locus, effectively decoupling nucleation and spreading. In these mutants, nucleation decayed slowly toward precold levels over the 20 days after cold. Concurrently, H3K36me3 levels and *FLC* expression increased (Fig. 1 and fig. S3), suggesting reversion of *FLC* loci from a nucleated and repressed state to an active expression state.

We then compared *FLC* dynamics in double mutants *clf lhp1*, *clf vrn2*, and *clf vin3*, with their respective single mutants, which indicated that LHP1 and CLF function in the same genetic pathway and that nucleation is upstream of spreading (Fig. 1A and fig. S1). Thus, VIN3/VRN2/VRN5–dependent H3K27me3 nucleation is required for *FLC* repression during the cold, and LHP1 and CLF are required after cold to mediate spreading of H3K27me3 for long-term stable silencing. With little or no spreading, H3K27me3 nucleation and silencing at *FLC* are maintained over ~20 days in *lhp1* and *clf*. Because plants are undergoing DNA replication, this suggests that the nucleated state alone can maintain a metastable epigenetic memory of silencing at *FLC*.

Mathematical models based on local inheritance of modified histones and cis-acting positive feedbacks had predicted that only the spread but not the nucleated state would be stable through DNA replication (*2*, *16*). We investigated the role of DNA replication by using the DNA synthesis inhibitor roscovitine (*17*). In *Arabidopsis*, root meristem cells in our warm conditions replicate their DNA approximately once per day (*18*). Roscovitine blocked cell division (fig. S4A), but this had no effect on *FLC* expression either before or after cold exposure in wild-type plants (fig. S4, B and C). By contrast, *FLC* reactivation normally seen in *clf* and *lhp1* mutants was reduced (Fig. 2A and fig. S4C), and H3K27me3 nucleation was stable (Fig. 2B). Inhibition of DNA synthesis impaired spreading of H3K27me3 in wild-type plants, even after 14 days of growth in the warm (Fig. 2B). These results suggest that DNA replication and/or cell division is required for the spreading of H3K27me3 and for the reactivation of *FLC* expression in *clf* and *lhp1* mutants.

To investigate this metastability at the single-cell level, we crossed the fluorescent *FLC-VENUS* reporter (*1*) to *vin3*, *vrn2*, and *lhp1*. We then combined confocal microscopy and quantitative image analysis (fig. S5) to determine FLC-VENUS levels in root meristems. Before cold exposure, FLC-VENUS is observed in all cells (fig. S6A). After cold exposure and subsequent growth in the warm for 7 days, wild-type plants showed long files of cells in either the ON or OFF expression states (Fig. 3A). These files demonstrate epigenetic maintenance of ON or OFF expression states because they are cell lineages generated through anticlinal cell divisions from progenitors that experienced cold exposure (*1*). In the nucleation mutants *vin3* and *vrn2*, FLC-VENUS remained ON in all cells. In the spreading mutant *lhp1*, FLC-VENUS showed the wild-type ON/OFF distribution (Fig. 3, A and B, and fig. S6, B and C). Thus, nucleation is itself an all-or-nothing process (*14*), and *FLC* repression is maintained through cell division in the *lhp1* mutant for at least 7 days after cold. To further test the stability of the silenced state in *lhp1*, we exposed plants to an extended 10-week cold treatment. After 14 days of subsequent growth in warm conditions, we observed the reappearance of a population of active cells that did not occur in wild-type plants (Fig. 3, C and D, and fig. S7). These *FLC*-ON cells often occurred as isolated cells or as short files that likely represent clonal propagation of cells that stochastically

[1]Department of Cell and Developmental Biology, John Innes Centre, Norwich Research Park, Norwich NR4 7UH, UK. [2]Department of Computational and Systems Biology, John Innes Centre, Norwich Research Park, Norwich NR4 7UH, UK. *These authors contributed equally to this work. †**Corresponding author. Email: martin.howard@jic.ac.uk (M.H.); caroline.dean@jic.ac.uk (C.D.)**

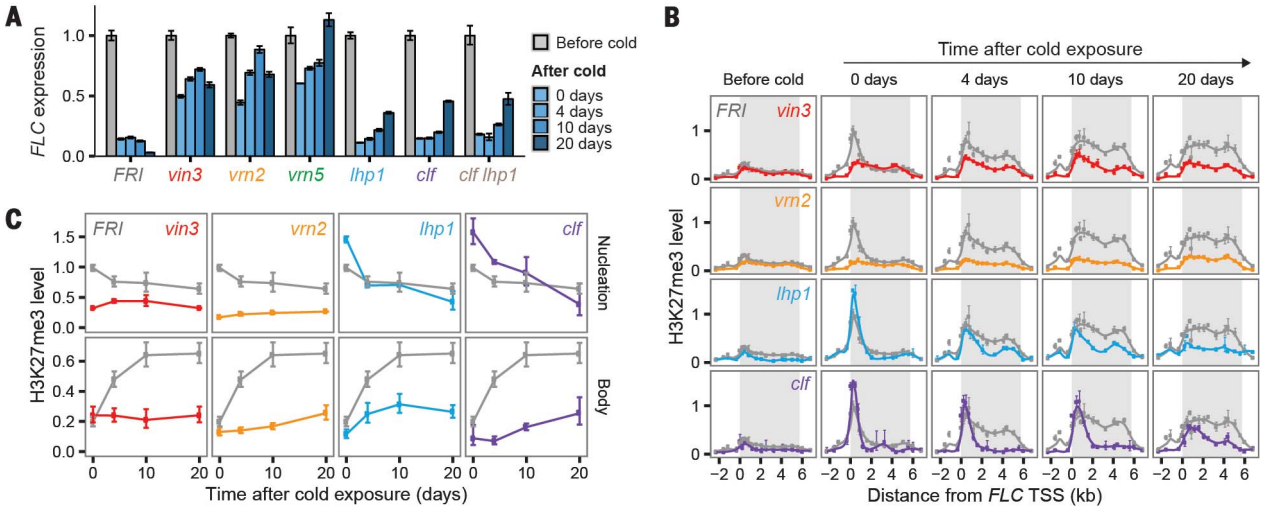

Fig. 1. Nucleation and spreading are genetically separable. (**A**) *FLC* expression measured with quantitative reverse transcription polymerase chain reaction after a 6-week cold treatment. Data are represented relative to *UBC*, with different genotypes normalized to nonvernalized *FLC* levels. Error bars represent SEM ($n \geq 3$ biological replicates). (**B**) H3K27me3 ChIP across the *FLC* locus before cold and after a 6-week cold treatment. Data are expressed relative to *SHOOT MERISTEMLESS* (*STM*). Error bars represent SEM ($n \geq 3$ biological replicates). Curves are fitted by using locally weighted scatterplot smoothing (LOESS) regression (supplementary materials). (**C**) H3K27me3 ChIP data averaged over two primers in the *FLC* nucleation region and five primers in the gene body (table S1). Error bars represent SD.

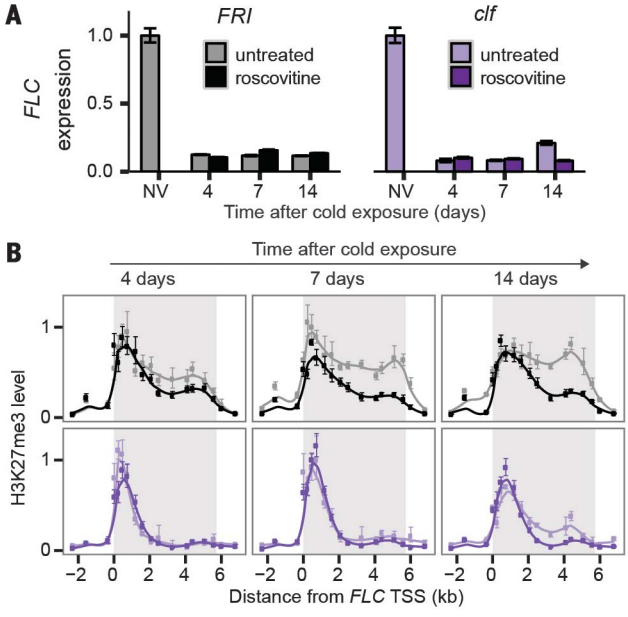

Fig. 2. Nucleation is maintained but spreading is inhibited by roscovitine treatment. (**A**) *FLC* expression after 6 weeks of cold in wild-type (*FRI*) or a *clf* mutant, with or without subsequent roscovitine treatment in warm conditions. Data are represented relative to *UBC*, with each genotype normalized to its respective nonvernalized (NV) *FLC* level. Error bars represent SEM ($n = 4$ biological replicates). (**B**) H3K27me3 levels at *FLC* after 6 weeks of cold, with or without subsequent roscovitine treatment in warm conditions. Data are expressed relative to *STM*. Error bars represent SEM ($n \geq 3$ biological replicates). Dark shades (black and purple) represent roscovitine treatment, whereas light shades (gray and light purple) represent untreated samples. Curves are fitted by using LOESS regression (supplementary materials).

reactivate *FLC* expression. These data agree with population-level mRNA and ChIP measurements, suggesting that the time scales of reactivation observed at the population level in *lhp1* mutants represent reactivation of *FLC* expression at the single-cell level. These findings further support the conclusion that LHP1 is not required for nucleation or for the propagation of metastable epigenetic memory.

To explore whether this metastable epigenetic memory is stored in the local chromatin environment of *FLC* (*1*), we generated *lhp1* plants that carry a single copy of *FLC-Venus* and *FLC-mCherry*. Before cold, FLC-Venus and FLC-mCherry were expressed in all root cells (fig. S8, A and B), whereas after cold, all four possible combinations of FLC-Venus/FLC-mCherry levels were found: ON/ON, ON/OFF, OFF/ON, and OFF/OFF (Fig. 3E and figs. S8 and S9). In both the wild-type and *lhp1* backgrounds, all expression states occurred in files, indicating that the epigenetic state of the two *FLC* copies in the same cell can be independently inherited. These data demonstrate that the metastable epigenetic memory of *FLC* silencing is stored in cis at the *FLC* locus not only in the wild type (*1*) but also in the spreading mutant, *lhp1*.

Our previous models of vernalization-induced epigenetic silencing at *FLC* have been based on inheritance of local histone modifications to daughter strands at DNA replication, followed by locally acting positive feedbacks to add similar modifications to newly incorporated histones (*2*, *16*). Such models require large chromatin regions to ensure that the chromatin state can be faithfully inherited despite random partitioning of nucleosomes during DNA replication. Spreading of H3K27me3 to the gene body (30 to 35 nucleosomes) fulfilled this requirement (*2*). Although this mechanism can explain long-term epigenetic memory at *FLC* in wild type, difficulties arise in accounting for the metastable silencing of *FLC* through DNA replication seen in *lhp1* and *clf* mutants, where H3K27me3 does not accumulate to high levels outside the nucleation region. Assuming that memory is only held in a nucleation region with three nucleosomes, the predicted dynamics would lead to a faster loss of silencing, with almost one quarter of diploid cells reactivating at least one *FLC* copy after each DNA replication (supplementary materials). Such rapid dynamics predict 75% reactivation within a week and are therefore inconsistent with the observed stability of *FLC* silencing in *lhp1* mutants (fig. S10). These conclusions are substantially unaffected, even if we allow for a low level of H3K27me3 spreading,

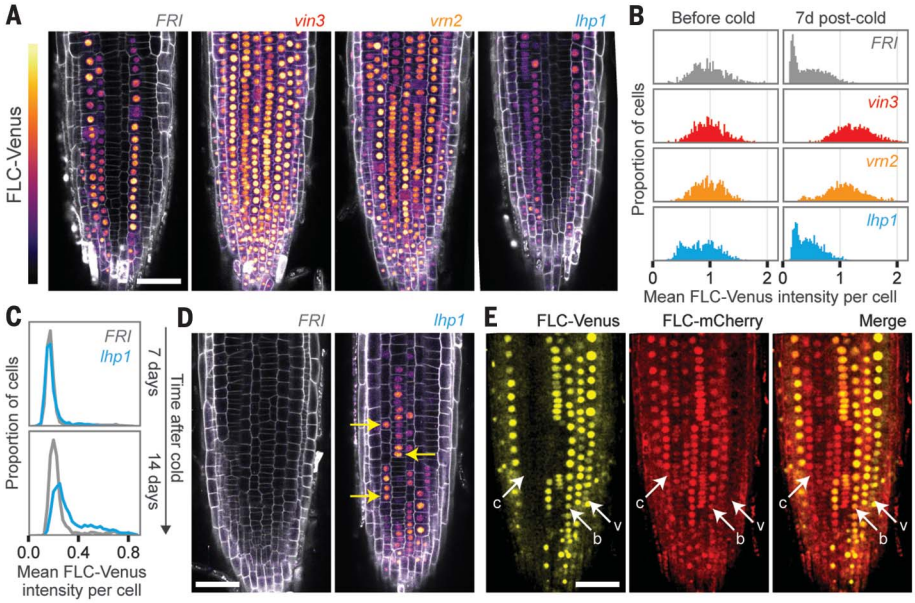

Fig. 3. "Metastable" cis epigenetic memory of *FLC* expression. (**A**) FLC-Venus intensity in root meristems in the wild-type and the various mutant backgrounds indicated. Plants were imaged 7 days after a 7-week cold treatment. (**B**) Histograms of single-cell FLC-Venus intensities obtained from automated image quantification, before cold and 7 days after a 7-week cold treatment. Numbers of roots and cells analyzed for each treatment are listed in table S2. (**C**) Distribution of single-cell FLC-Venus intensities in *FRI* and *lhp1*, 7 and 14 days after a 10-week cold treatment. Numbers of roots and cells analyzed for each treatment are listed in table S2. (**D**) FLC-Venus imaged 14 days after a 10-week cold treatment in the wild type and *lhp1* mutant. Arrows in *lhp1* plants indicate cells that show discontinuous expression relative to a neighboring cell of the same file. (**E**) FLC-Venus and FLC-mCherry intensities in root meristems 10 days after a 6-week cold treatment in the *lhp1* mutant. The following notation is used to indicate files of cells in the various expression states: Both expressed, b; FLC-Venus only, v; FLC-mCherry only, c. Scales bars in (A), (D), and (E), 50 μm.

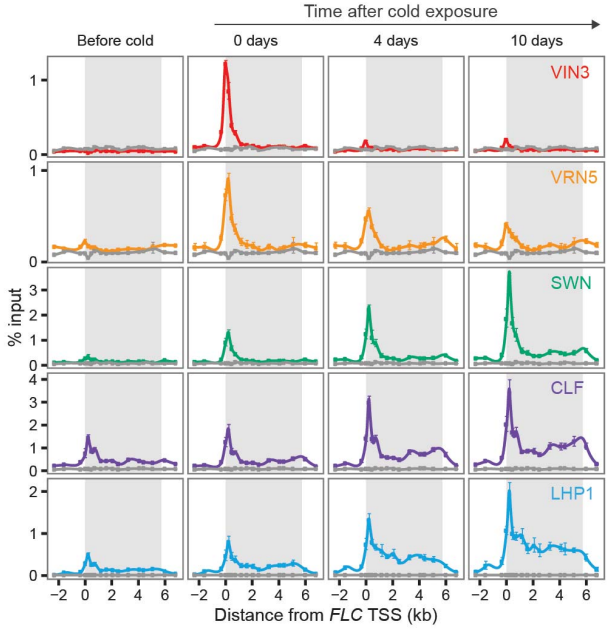

Fig. 4. Dynamics of protein occupancy during vernalization. ChIP for indicated tagged proteins across the *FLC* locus before cold and after a 6-week cold treatment. The nontransgenic plant *FRI* was used as background control (gray line). Error bars represent SEM (n = 3 biological replicates). Curves are fitted by using LOESS regression (supplementary materials).

as found in *lhp1* (supplementary materials, fig. S10, C and D). We therefore propose that additional protein factors present at the nucleation region may contribute directly in propagating metastable cis epigenetic memory, potentially through self-reinforcing protein-protein interactions stabilizing the retention of factors such as VRN5.

To address this hypothesis, we mapped the binding of VIN3, VRN5, SWN, CLF, and LHP1 [using *VIN3-GFP/vin3*, *VRN5-YFP/vrn5*, *SWN-YFP*, *35S::GFP-CLF/clf*, and *LHP1-eGFP/lhp1-6* (*10*, *19*–*21*)] at high spatial resolution across the *FLC* locus during vernalization. We verified that the newly generated *VIN3-GFP* and *LHP1-eGFP* constructs complemented their respective mutant phenotypes (figs. S11 and S12) and that *VIN3-GFP* showed a similar dynamic expression pattern as that of endogenous *VIN3* (fig. S11). We also verified that VRN5, SWN, CLF, and LHP1 tagged proteins localized to the nuclei, and that all the proteins including VIN3 could be efficiently enriched (figs. S11C; S12, F and G; and S13).

ChIP experiments indicated that VIN3, VRN5, and SWN were absent from the *FLC* locus before cold (Fig. 4 and fig. S14). During cold, VIN3 protein was targeted to the *FLC* nucleation region (Fig. 4). Similar to VIN3, localization of SWN and VRN5 during cold was limited to the *FLC* nucleation region. Together, these data indicate recruitment of VIN3/VRN5/SWN at the *FLC* nucleation region during cold exposure. After cold, however, the dynamics of these three proteins differed: VIN3 was lost within days; VRN5 was lost more slowly at the nucleation region over >10 days, but also exhibited low-level spreading over the gene body; whereas SWN occupancy increased when H3K27me3 spread to cover the *FLC* gene body. Levels of VIN3 at *FLC* correlated with the *VIN3* mRNA expression level and also with bulk levels of VIN3-GFP protein (Fig. 4 and fig. S11C). *VRN5*, *VRN2*, *SWN*, *CLF*, and *LHP1* were all more constitutively expressed (fig. S2, B to E) (*10*). These findings suggest that the cold-induced localization of VIN3 is essential to trigger nucleation and that dynamic changes in the localization of the other proteins at *FLC* during vernalization are unlikely to be driven by altered expression levels. The dynamics of VRN5 loss from the nucleation region after cold parallels the loss of H3K27me3 at the nucleation region in *lhp1*/*clf* mutants (Figs. 1, B and C, and 4 and fig. S15), suggesting that VRN5 defines the metastability of the nucleation-region memory.

To elaborate the mechanism underlying long-term epigenetic memory at *FLC*, we examined the dynamics of CLF and LHP1 in the different phases of vernalization. Both proteins showed similar levels at *FLC* during and after cold exposure: Both were associated with *FLC* chromatin before cold; showed limited increases during cold; and, similar to SWN, increased in occupancy at the nucleation region after cold (Fig. 4). LHP1 and CLF also showed more pronounced spreading to the gene body after cold than did SWN (Fig. 4), which is a feature consistent with their mutant phenotypes that show reduced H3K27me3 domain size at *FLC* and genome-wide (*22*, *23*). LHP1 and CLF physically interact through additional PRC2 components (*24*), and furthermore, both LHP1 and other PRC2 subunits bind H3K27me3 (*25*–*27*), so our observed colocalization of CLF and H3K27me3 suggests that CLF likely deposits H3K27me3 in the *FLC* gene body. These reading and writing functions of PRC2 and LHP1 for H3K27me3 may contribute to reinforcing

the repressive chromatin state in the *FLC* gene body, which is consistent with its long-term stability.

Our analysis of cold-induced epigenetic silencing at *FLC* clarifies the sequence of events involved in Polycomb silencing of a genomic locus. Specialized Polycomb components function in two phases of cis-inherited silencing that are genetically and mechanistically separate, to confer first reversible and then long-term epigenetic memory (fig. S16).

REFERENCES AND NOTES

1. S. Berry, M. Hartley, T. S. G. Olsson, C. Dean, M. Howard, *eLife* **4**, e07205 (2015).
2. A. Angel, J. Song, C. Dean, M. Howard, *Nature* **476**, 105–108 (2011).
3. L. Bintu *et al*., *Science* **351**, 720–724 (2016).
4. M. J. Obersriebnig, E. M. Pallesen, K. Sneppen, A. Trusina, G. Thon, *Nat. Commun.* **7**, 11518 (2016).
5. S. D. Michaels, R. M. Amasino, *Plant Cell* **11**, 949–956 (1999).
6. E. Jean Finnegan *et al*., *Plant J.* **44**, 420–432 (2005).
7. F. De Lucia, P. Crevillen, A. M. Jones, T. Greb, C. Dean, *Proc. Natl. Acad. Sci. U.S.A.* **105**, 16831–16836 (2008).
8. A. R. Gendall, Y. Y. Levy, A. Wilson, C. Dean, *Cell* **107**, 525–535 (2001).
9. S. Sung, R. M. Amasino, *Nature* **427**, 159–164 (2004).
10. T. Greb *et al*., *Curr. Biol.* **17**, 73–78 (2007).
11. J. S. Mylne *et al*., *Proc. Natl. Acad. Sci. U.S.A.* **103**, 5012–5017 (2006).
12. S. Sung *et al*., *Nat. Genet.* **38**, 706–710 (2006).
13. H. Yang, M. Howard, C. Dean, *Curr. Biol.* **24**, 1793–1797 (2014).
14. A. Angel *et al*., *Proc. Natl. Acad. Sci. U.S.A.* **112**, 4146–4151 (2015).
15. W. Yuan *et al*., *Nat. Genet.* **48**, 1527–1534 (2016).
16. I. B. Dodd, M. A. Micheelsen, K. Sneppen, G. Thon, *Cell* **129**, 813–822 (2007).
17. S. Planchais *et al*., *Plant J.* **12**, 191–202 (1997).
18. G. V. Reddy, M. G. Heisler, D. W. Ehrhardt, E. M. Meyerowitz, *Development* **131**, 4225–4237 (2004).
19. J. I. Qüesta, J. Song, N. Geraldo, H. An, C. Dean, *Science* **353**, 485–488 (2016).
20. D. Schubert *et al*., *EMBO J.* **25**, 4638–4649 (2006).
21. D. Wang, M. D. Tyson, S. S. Jackson, R. Yadegari, *Proc. Natl. Acad. Sci. U.S.A.* **103**, 13244–13249 (2006).
22. H. Wang *et al*., *PLOS Genet.* **12**, e1005771 (2016).
23. A. Veluchamy *et al*., *PLOS ONE* **11**, e0158936 (2016).
24. M. Derkacheva *et al*., *EMBO J.* **32**, 2073–2085 (2013).
25. C. Xu *et al*., *Proc. Natl. Acad. Sci. U.S.A.* **107**, 19266–19271 (2010).
26. K. H. Hansen *et al*., *Nat. Cell Biol.* **10**, 1291–1300 (2008).
27. X. Zhang *et al*., *Nat. Struct. Mol. Biol.* **14**, 869–871 (2007).

ACKNOWLEDGMENTS

We thank H. Wang for technical help, S. Chen for plant handling, J. Goodrich for *35S::GFP-CLF/clf-28* seeds, G. Calder for microscopy support, and members of the C.D. and M. Howard research groups for discussions. The project was supported by European Research Council grants 233039 and 339462 and by the UK Biotechnology and Biological Sciences Research Council Institute Strategic Programme grant BB/J004588/1. S.B. was supported by a John Innes Foundation studentship. Additional data are provided in the supplementary materials.

SUPPLEMENTARY MATERIALS

www.sciencemag.org/content/357/6356/1142/suppl/DC1
Materials and Methods
Figs. S1 to S16
Tables S1 and S2
References (*28*–*47*)

6 March 2017; resubmitted 27 April 2017
Accepted 29 June 2017
Published online 17 August 2017
10.1126/science.aan1121

Distinct phases of Polycomb silencing to hold epigenetic memory of cold in *Arabidopsis*

Hongchun Yang, Scott Berry, Tjelvar S. G. Olsson, Matthew Hartley, Martin Howard and Caroline Dean

Science **357** (6356), 1142-1145.
DOI: 10.1126/science.aan1121originally published online August 17, 2017

Managing gene silencing through replication

Vernalization is the process in plants by which wintertime chill stimulates springtime flowering. Yang *et al.* and Jiang *et al.* show how chill is recorded in *Arabidopsis* epigenetically by methylation of histones. Specialized components of the Polycomb group of proteins remodel DNA to establish the methylation marks and are linked to DNA replication. Long-term stable epigenetic status follows rapid establishment of metastable epigenetic marks. This epigenetic strategy may be key to the developmental requirement of both secure and nimble fate decisions, allowing plant cells to change fates.

Science, this issue p. 1142 and p. 1146